

SPEED RESPONSE AND ELECTROMAGNETIC TORQUE CHARACTERISTICS ANALYSIS OF THREE-PHASE INDUCTION MOTOR USING THYRISTOR-CONTROLLED METHOD

Tochukwu Daniel Echeme^{*1}, Christopher Victor Onwukwe², Anthony Jacob Eke³,
Cyprian Izuchukwu Igwedibia⁴

¹Department of Electrical and electronic Engineering, University of Agriculture and
Environmental Sciences, Umuagwo, Nigeria.

²Department of Electrical and Electronic Engineering, Federal Polytechnic Nekede, Owerri,
Nigeria.

³Department of Electrical and Electronic Engineering, Federal Polytechnic Ngodo, Isuochi,
Nigeria.

⁴Department of Electrical and Electronic Engineering, Imo State University, Owerri, Nigeria.

Article Received: 04 January 2026

*Corresponding Author: Tochukwu Daniel Echeme

Article Revised: 24 January 2026

Department of Electrical and electronic Engineering, University of Agriculture and

Published on: 12 February 2026

Environmental Sciences, Umuagwo, Nigeria.

DOI: <https://doi-doi.org/101555/ijrpa.4183>

ABSTRACT:

This paper presents speed response and electromagnetic torque characteristics analysis of three-phase induction motor using thyristor-controlled method. Modelling, implementation, and testing of a thyristor-controlled three-phase induction motor system were carried out using MATLAB/Simulink to performed numerical and computer simulation analysis. Simulation was successfully conducted under four different loading conditions (0, 5, 10, and 20 N-m), and comprehensive performance data was collected and analysed. The results demonstrated that: the system exhibited stable operation across all tested load conditions. An obvious observation was that the dynamic performance degrades progressively with increasing load, and the controller maintains adequate speed regulation despite varying mechanical loading.

KEYWORDS: Three-phase induction motor, Thyristor-controlled method, Speed control, Electromagnetic torque.

1. INTRODUCTION

Induction motors are type of electric derives (machines) that are widely employed in industrial applications. Nearly more than half of the overall electrical energy produced in industry is used by electric machines (Marulasiddappa & Viswanathan, 2020). The electric machines used in the industries consist of direct current (DC) motors, induction motors, synchronous motors and others. In industries, more than 70% of electrical energy are consumed are used by motors and as such, energy together with operating cost, can be saved by improving electric motors' efficiency (Gupta, 2021). Induction motors have eventually taken over the place of other types of electric drives because of their low cost compare to other motors, inherent robustness, better reliability and ability to produce better efficiency (Rahman & Bin ZainalAbidin, 2016; Marulasiddappa & Viswanathan, 2020).

Three phase induction motor is largely used in industrial sector due to its ruggedness and reliability (Rahman & Bin ZainalAbidin, 2016). However, single phase induction motor is used in household equipment such as fan. Induction motor is largely employed in industrial appliances rather than DC motors because it can offer a high-speed torque response (Guohanin & Xu, 2010; Latt & Win, 2009). Different kinds of operation and various multiple speed functions are performed by speed control of induction motor. Several methods of control have been used to regulate the speed of induction of induction motor, which includes conventional control methods such as frequency control, voltage control (Chandrasekhari & Sindhuja, 2014) and more recent types involving the use of predictive control, intelligent control.

Despite its merits, induction motor also has some drawbacks. Its dynamic characteristics are highly complex. Thus, the modelling of induction motor results in system of non-linear, strongly coupled and multivariable equation. In addition, induction motor speed control is difficult due to its nonlinearity. Research is still being carried out on speed control of induction motor (Marulasiddappa & Viswanathan, 2020) and the most commonly used method is the classical controllers (PI and PID) and fuzzy logic controller as in Idoko et al. (2017), Korsane et al. (2018), Hartono et al. (2019), Irianto et al. (2021), and Singh et al. (2021).

This work presents the design, implementation, and testing of the thyristor-controlled three-phase induction motor system using thyristor. The system was modelled and simulated using MATLAB Simulink to evaluate the performance characteristics of the motor under various

operating conditions. The primary objective was to analyse the speed response and electromagnetic torque behaviour of the motor at different load torques.

2. SYSTEM DESIGN

This chapter presents the design, implementation, and testing of the thyristor-controlled three-phase induction motor system. The system was modelled and simulated using MATLAB Simulink to evaluate the performance characteristics of the motor under various operating conditions. The primary objective was to analyse the speed response and electromagnetic torque behaviour of the motor at different load torques.

2.1 Design Specifications and Block Diagram

The system was designed with the following specifications:

- Motor Type: Three-phase squirrel cage induction motor
- Control Method: Thyristor-based voltage control
- Operating Speed: Variable speed operation
- Load Conditions: 0, 5, 10, and 20 N-m

The overall system configuration consists of the following main components:

- Three-phase AC power supply
- Thyristor converter circuit
- Gate pulse generation unit
- Three-phase induction motor
- Load torque application
- Measurement and monitoring systems

The block diagram illustrates the complete system architecture, comprising:

- Input Side: Three-phase AC voltage source (V_{an} , V_{bn} , V_{cn}) providing balanced sinusoidal voltages
- Thyristor Bridge: Six thyristors (S1-S6) configured in a three-phase bridge converter topology with individual gate signal controls ($|S1|$ through $|S6|$)
- Triggering Pulses: Pulse generation circuit producing synchronized gate signals (G1-G6) for precise firing angle control
- Induction Motor: Three-phase induction motor with stator terminals (A, B, C) connected to the converter output
- Load Application: Mechanical load block connected to the motor shaft

- Measurement System: Rotor speed and electromagnetic torque sensors with display units for real-time monitoring
- Control System: Continuous-time simulation block coordinating the overall system operation.

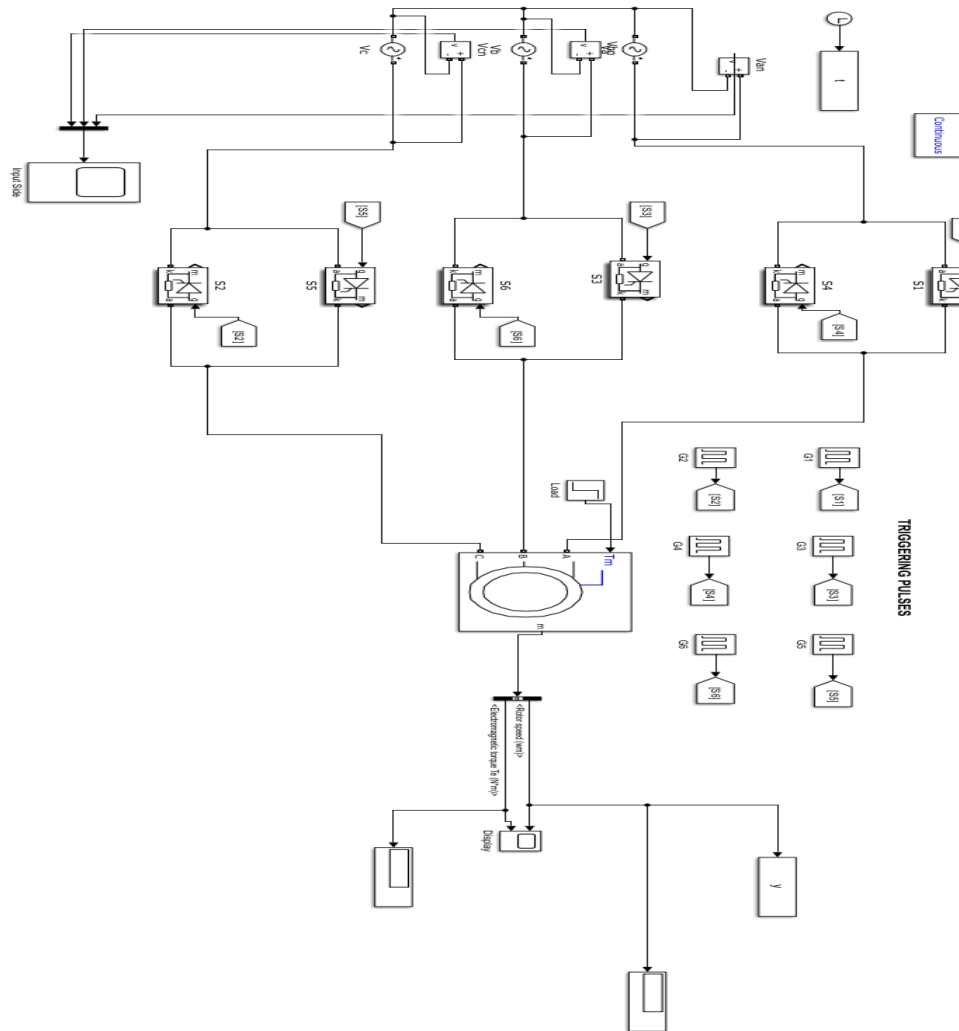


Figure 1: Simulink block diagram of thyristor-controlled three-phase induction motor system.

The thyristor-controlled three-phase induction motor system was implemented using MATLAB Simulink, which provides a comprehensive platform for modeling, simulation, and analysis of power electronic and motor drive systems. The Simulink model was developed by integrating various blocks from the Simscape Electrical library and standard Simulink libraries. The complete system model is shown in Figure 1, which depicts the interconnection of all major subsystems. The implementation involved:

1. Power Supply Configuration: A three-phase voltage source was configured to provide balanced sinusoidal voltages (V_{an} , V_{bn} , V_{cn}) to the thyristor converter. Figure 2 shows the three-phase AC supply voltage waveforms, demonstrating the 120° phase displacement between the three phases. The voltages exhibit clean sinusoidal characteristics with peak amplitudes of approximately $\pm 240V$.

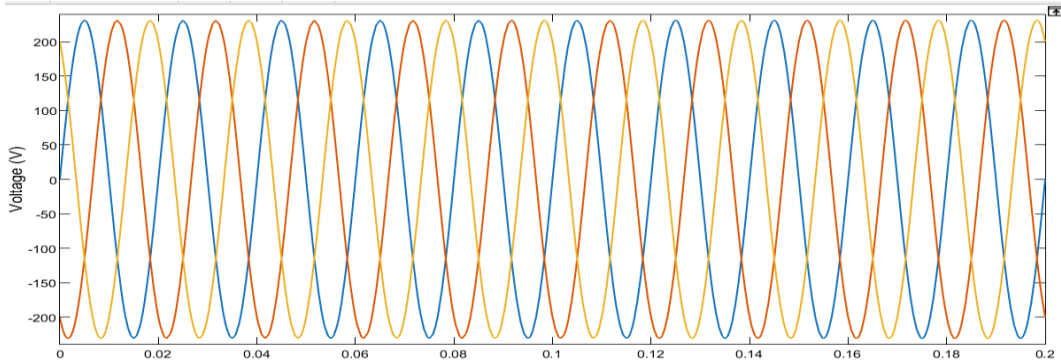


Figure 2: Three-Phase AC Supply Voltage (Van - Blue, Vbn - Orange, Vcn - Yellow).

2. Thyristor Converter Design: The thyristor-based converter was implemented using a six-pulse bridge rectifier topology consisting of thyristors S1 through S6. Each thyristor is equipped with individual gate signal inputs ($|S1|$ to $|S6|$) for independent control of the firing angles.

3. Gate Pulse Generation: A firing angle control scheme was implemented through the triggering pulses subsystem, which generates appropriate gate pulses (G1 through G6) for the thyristors. The pulse generation circuit ensures proper sequential firing of the thyristors to maintain balanced three-phase operation and prevent commutation failures.

4. Induction Motor Model: The three-phase induction motor was modeled using the standard machine parameters including stator resistance, rotor resistance, mutual inductance, and moment of inertia. The motor terminals (A, B, C) are directly connected to the output of the thyristor bridge converter.

5. Load Torque Application: A variable load torque block was incorporated to simulate different loading conditions on the motor shaft, enabling the evaluation of system performance under varying mechanical loads.

6. Measurement Systems: Rotor speed and electromagnetic torque measurement blocks were integrated to capture the system's dynamic response. These measurements are displayed in real-time through dedicated display units and output to the workspace for further analysis.

3. RESULTS AND DISCUSSION

The performance of the thyristor-controlled three-phase induction motor system was evaluated by varying the load torque at 0, 5, 10, and 20 N-m. For each loading condition, the motor speed and electromagnetic torque responses were analyzed, and key transient response parameters were extracted.

3.1 Speed Performance at No Load

In this condition, it was assumed that the motor is running at no load (i.e., Load Torque = 0 N-m). Figure 3 shows the simulated speed and electromagnetic torque of the motor at no load.

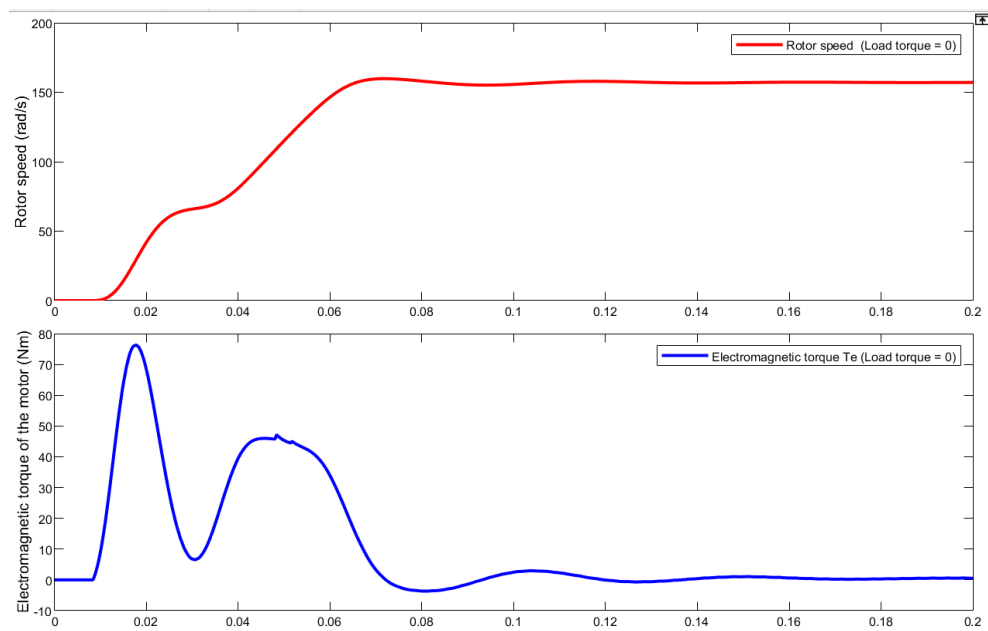


Figure 3: Speed and Electromagnetic Torque at No Load (0 N-m)

From the simulated plots in Figure 3, the transient response performance of the motor speed at no load is presented in Table 1.

Table 1: Transient Response Parameters at No Load (0 N-m)

Parameter	Value
Rise Time	0.0428 s
Transient Time	0.0635 s
Settling Time	0.0635 s
Overshoot	1.7316%
Peak	159.8005 rad/s
Peak Time	0.0717 s

The results indicates that the motor exhibits excellent starting characteristics at no load, with minimal overshoot and a relatively fast settling time. The motor reached its peak speed of 159.8005 rad/s within 0.0717 seconds, demonstrating a rapid acceleration profile.

3.2 Speed Performance at 5 N-m Load

When a load torque of 5 N-m is applied to the motor shaft, the speed and electromagnetic torque characteristics changed as shown in Figure 4.

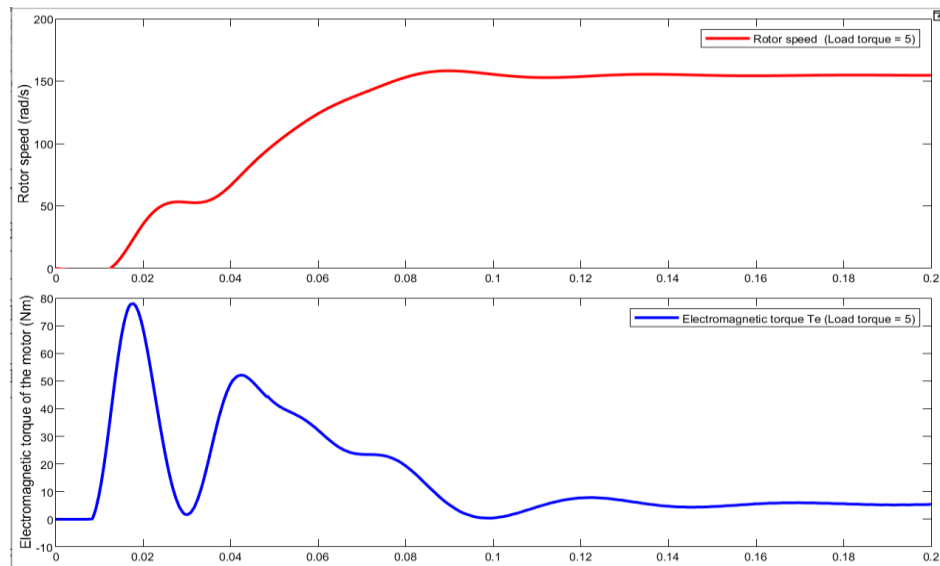


Figure 4: Speed and Electromagnetic Torque at 5 N-m Load.

The transient response parameters for the motor operating under 5 N-m load are summarized in Table 2.

Table 2: Transient Response Parameters at 5 N-m Load.

Parameter	Value
Rise Time	0.0530 s
Transient Time	0.0932 s
Settling Time	0.0935 s
Overshoot	2.3539%
Peak	158.2393 rad/s
Peak Time	0.0896 s

As observed from the results, the application of a 5 N-m load caused a slight increase in the rise time to 0.0530 seconds and settling time to 0.0935 seconds. The overshoot increased marginally to 2.3539%, while the peak speed decreased to 158.2393 rad/s. This behavior is expected as the motor must overcome the additional load torque, resulting in slightly degraded dynamic performance compared to the no-load condition.

3.3 Speed Performance at 10 N-m Load

With a further increase in load torque to 10 N-m, the motor's speed and torque responses are illustrated in Figure 5.

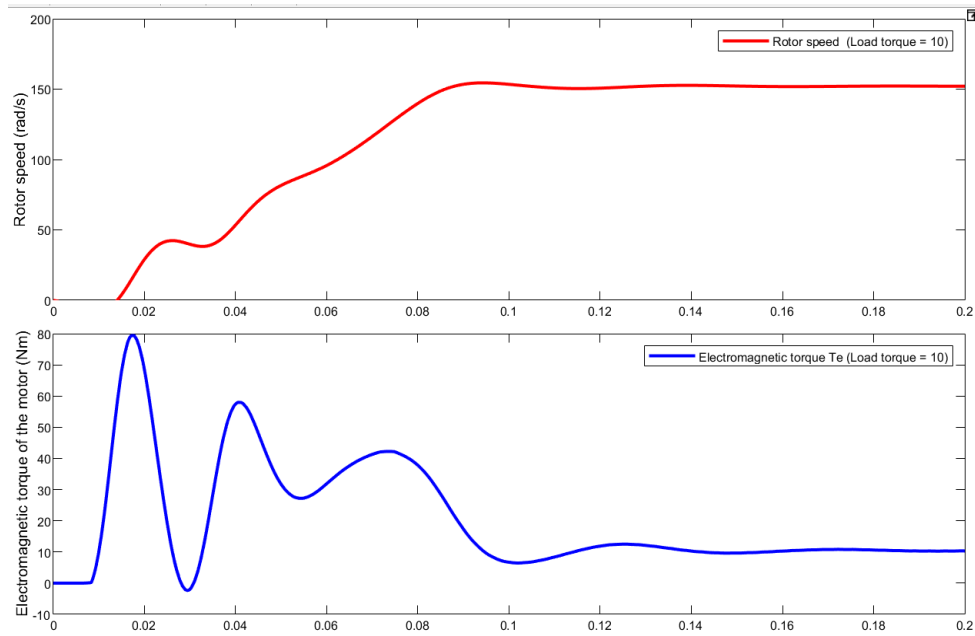


Figure 5: Speed and Electromagnetic Torque at 10 N-m Load.

Table 3 presents the transient response characteristics of the motor under 10 N-m loading condition.

Table 3: Transient Response Parameters at 10 N-m Load

Parameter	Value
Rise Time	0.0613 s
Transient Time	0.0851 s
Settling Time	0.0852 s
Overshoot	1.5828%
Peak	154.4486 rad/s
Peak Time	0.0942 s

The results indicated that at 10 N-m load, the motor exhibited a rise time of 0.0613 seconds and a settling time of 0.0852 seconds. Interestingly, the overshoot decreased to 1.5828% while the undershoot increased to 4.6302. The peak speed further reduced to 154.4486 rad/s, reflecting the impact of increased mechanical loading on the motor's operating speed.

3.4 Speed Performance at 20 N-m Load

At the maximum test load of 20 N-m, the motor's performance characteristics are shown in Figure 6.

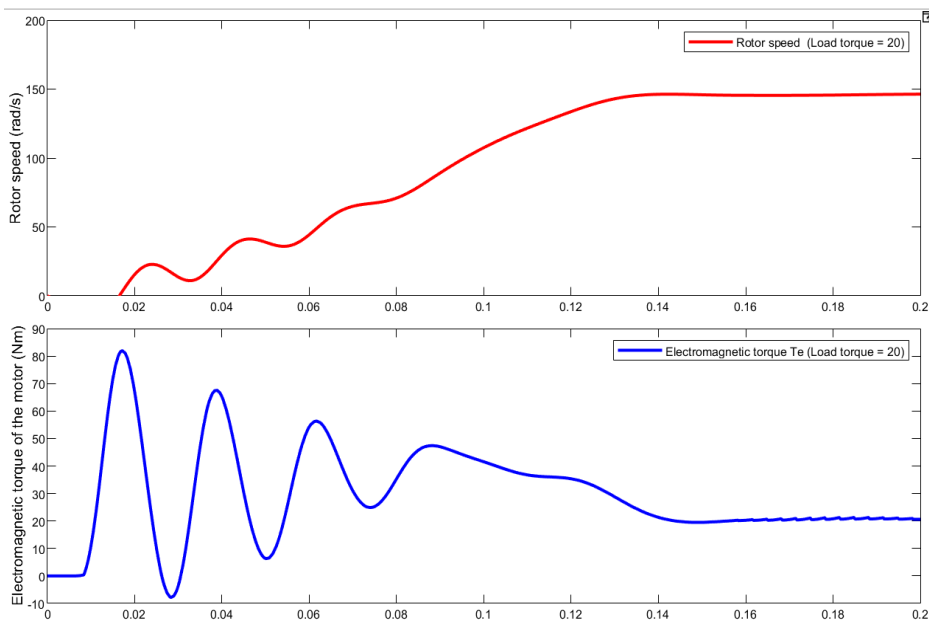


Figure 6: Speed and Electromagnetic Torque at 20 N-m Load.

The transient response parameters for the heavily loaded motor are presented in Table 4.

Table 4: Transient Response Parameters at 20 N-m Load

Parameter	Value
Rise Time	0.0985 s
Transient Time	0.1302 s
Settling Time	0.1307 s
Overshoot	0%
Peak	146.3196 rad/s
Peak Time	0.2000 s

Under the 20 N-m load condition, the motor demonstrates significantly different dynamic characteristics. The rise time increases substantially to 0.0985 seconds, with the settling time extending to 0.1307 seconds. Notably, there is no overshoot observed, indicating a critically damped or overdamped response. The undershoot increases dramatically to 10.1534, and the steady-state speed drops to 146.3196 rad/s, which represents the expected speed reduction under heavy loading conditions.

3.5 Comparative Analysis

A comparative analysis of the motor performance across different loading conditions reveals several important trends:

- Speed Reduction:** As the load torque increases from 0 to 20 N-m, the steady-state peak speed decreases from 159.8005 rad/s to 146.3196 rad/s, representing an approximately 8.4% reduction in operating speed.
- Rise Time Variation:** The rise time increases progressively with load, more than doubling from 0.0428 seconds at no load to 0.0985 seconds at 20 N-m load.
- Settling Time:** Similarly, the settling time increases from 0.0635 seconds to 0.1307 seconds as the load increases, indicating slower transient response under heavier loading.
- Overshoot Characteristics:** The overshoot initially increases from 1.7316% to 2.3539% as the load increases from 0 to 5 N-m, but then decreases to 1.5828% at 10 N-m and eventually reaches 0% at 20 N-m, suggesting a transition from under-damped to critically damped behavior.

The simulation results demonstrate that the thyristor-controlled three-phase induction motor system exhibits predictable and stable performance across a wide range of loading conditions. The controller successfully maintains motor operation at all tested load levels, though with expected degradation in dynamic performance as the load increases.

The progressive increase in rise time and settling time with increasing load is characteristic of induction motor behavior, where the electromagnetic torque must overcome both the inertia of the rotor and the applied load torque. The reduction in steady-state speed with increasing load is consistent with the speed-torque characteristic of induction motors operating below synchronous speed.

The absence of overshoot at the highest load condition (20 N-m) suggests that the system becomes more heavily damped under significant mechanical loading, which is generally desirable from a stability perspective, though it results in slower response times.

4. CONCLUSION

In this work, design, implementation, and testing of a thyristor-controlled three-phase induction motor system using MATLAB Simulink has been carried out. The system was successfully simulated under four different loading conditions (0, 5, 10, and 20 N-m), and comprehensive performance data was collected and analyzed. The results demonstrate that: The system exhibits stable operation across all tested load conditions, dynamic performance degrades progressively with increasing load, and the controller maintains adequate speed regulation despite varying mechanical loading.

REFERENCES

1. Chandrasekhari, J., & Sindhuja, S. (2014). A fuzzy based speed controller for induction motor drive. *Communications in Differential and Difference Equations*, 5(1), 51-59.
2. Guohanin, & Xu, Z. (2010). Direct torque control of induction motor based on fuzzy *Proceeding of the International Conference on Computer Engineering Technology*, 4, 651 – 654.
3. Gupta, P. K. (2021). Action Plan Report on Squirrel Cage Induction Motor for Import Reduction and Promoting Domestic Manufacturing in MSME. https://dcmsme.gov.in/17_Squirrel%20Cage%20Induction%20Motor%20by%20PK%20Gupta.pdf
4. Hartono, H., Sudjoko, R. I., & Iswahyudi, P. (2009). Speed control of three phase induction motor using universal bridge and PID controller. *Journal of Physics: Conference Series*, 1381, 012053. <http://dx.doi.org/10.1088/1742-6596/1381/1/012053>
5. Idoko, A. A., Thuku, I. T., Musa, S. Y., & Amos, C. (2017). Design of tuning mechanism of PID controller for application in three phase induction motor speed control. *International Journal of Advanced Engineering Research and Science*, 4(11), 138 – 146. <https://dx.doi.org/10.22161/ijaers.4.11.21>
6. Irianto, Murdianto, F. D., Sunarno, E., & Proboningtyas, D. D. (2021). Comparison method of PI, PID, and fuzzy logic controller to maintain speed stability in single phase induction motors. *INTEK Jurnal Penelitian*, 8(1), 7 – 16. <http://dx.doi.org/10.31963/intek.v8i1.2687>
7. Korsane, D. T., Polke, A., Mude, S. K., Hiwarkar, C. S., Korsane, K. (2018). Speed performance of three phase induction motor by using simplified vector control method. *International Journal of Engineering Research in Electrical and Electronic Engineering*, 4(3), 172 – 178.
8. Latt, A. Z., & Win, N. N. (2009). Variable speed drive of single phase induction motor using frequency control method. *International Conference on Education Technology and Computer*, 65 – 71.
9. Marulasiddappa, H. B., & Viswanathan, P. (2020). A review paper on various control techniques for induction motor drives. *International Journal of Advanced Science and Technology*, 29(6), 6831-6837.

10. Rahman, S., & and Bin Zainal Abidin, A. A. (2016). A review on induction motor speed control methods. *International Journal of Core Engineering & Management*, 3(5), 116 – 124.
11. Singh, A., Singh, D. D., & Yadav, A. (2021). FLC based speed control of induction motor. *Journal of Physics: Conference Series*, 2007, 012020. <https://doi.org/10.1088/1742-6596/2007/1/012020>